

# Synthesis of Poly(GG-co-AAm-co-MAA), a Terpolymer Hydrogel for the Removal of Methyl Violet and Fuchsin Basic Dyes from Aqueous Solution

Shahid Khan, Najeeb Ur Rahman, Sultan Alam, Muhammad Zahoor,\* Luqman Ali Shah, Muhammad Naveed Umar, and Riaz Ullah



Cite This: *ACS Omega* 2024, 9, 7692–7704



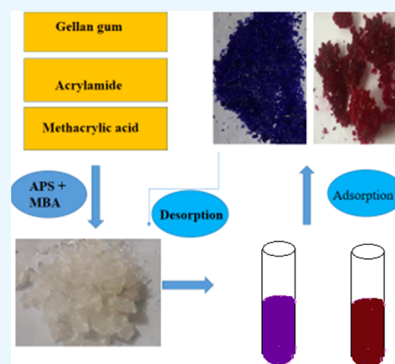
Read Online

ACCESS |

Metrics & More

Article Recommendations

**ABSTRACT:** A novel adsorbent designated as terpolymer hydrogel (gellan gum-co-acrylamide-co-methacrylic acid) was prepared by free radical polymerization of gellan gum (GG), methacrylic acid (MAA), and acrylamide (AAm) using *N,N*-methylene bis-acrylamide (MBA) as cross-linker and ammonium per sulfate (APS) as the initiator of the reaction. The synthesized gel was characterized by scanning electron microscopy (SEM), Fourier-transform infrared spectroscopy (FTIR), X-ray diffraction (XRD), Brunauer–Emmett–Teller (BET), and thermogravimetric analysis (TGA) and was used for the adsorptive removal of methyl violet (MV) and Fuchsin Basic (FB) dyes from aqueous solution. The effect of temperature, contact time, pH, and concentration on them under the study adsorption process was evaluated. Freundlich isotherm and pseudo-second-order kinetic models were found to be best in fitting the isothermal and kinetics data. The water diffusion and % swelling of hydrogel were studied at various pH in distilled water and at neutral pH in tap water. The diffusion was found to be of Fickian type with a maximum swelling of 5132%. The maximum adsorption capacity was 233 mg/g against MV and 200 mg/g against FB dyes. The swelling and adsorption were pH dependent and increased with increase in pH. The enthalpy, Gibbs free energy, and entropy changes of adsorption for both the dyes indicated the adsorption process to be exothermic, feasible, and spontaneous. The hydrogel was successfully regenerated using acetone and distilled water for five cycles and still, its dye removal efficiency was 80% of its original value. The poly(GG-co-AAm-co-MAA) hydrogel successfully removed the selected dyes from water and could thus be used as an efficient alternative sorbent for cationic dye removal from aqueous solutions.



## 1. INTRODUCTION

Hydrogels are three-dimensional, cross-linked networks with an incredible capacity to absorb and hold large amounts of water molecules without undergoing dissolution or alterations in their shapes. This fact makes it unique from conventional absorbents like cotton, sponges, and colloidal silica.<sup>1</sup> The inherent softness, hydrophilic nature, porosity, and elasticity of these materials make them suitable for various applications like hygienic products, agricultural applications, environmental remediation, wastewater treatment, and controlled drug delivery systems.<sup>2,3</sup> Nowadays, large numbers of super-absorbents are available for many applications, but due to their high manufacturing cost and nonecofriendly nature, they are not the material of choice. Therefore, a need is felt to synthesize superabsorbents based on natural polysaccharides like Gellan gum having properties like biocompatibility, biodegradability, and nontoxicity.<sup>4,5</sup> Gellan gum (GG) is a biopolymer (polysaccharide) produced by bacteria known as *Pseudomonas elodea*,<sup>6</sup> containing numerous hydrophilic groups.<sup>7</sup> Copolymerization of GG with materials such as acrylamide (AAm) and methacrylic acid (MAA) offers the

opportunity to enhance the properties of Gellan gum. These copolymer hydrogels exhibit novel functionalities and characteristics like thermal stability<sup>8,9</sup> as well as high adsorption capacities.<sup>10</sup>

Currently, many industries like pharmaceutical, food, textile, paper, cosmetic, and pulp use synthetic dyes for fixing and dyeing purposes, where some part of these are released into water bodies.<sup>11</sup> Most of the discharged dyes are highly water-soluble<sup>12</sup> and cause water pollution. Water pollution is a global problem because it causes diseases and in severe cases can cause death. According to an estimate, 14,000 people die every year due to water pollution.<sup>13,14</sup> The harmful effects of dyes are respiratory problems like asthma, coughing, and wheezing; it

**Received:** September 17, 2023

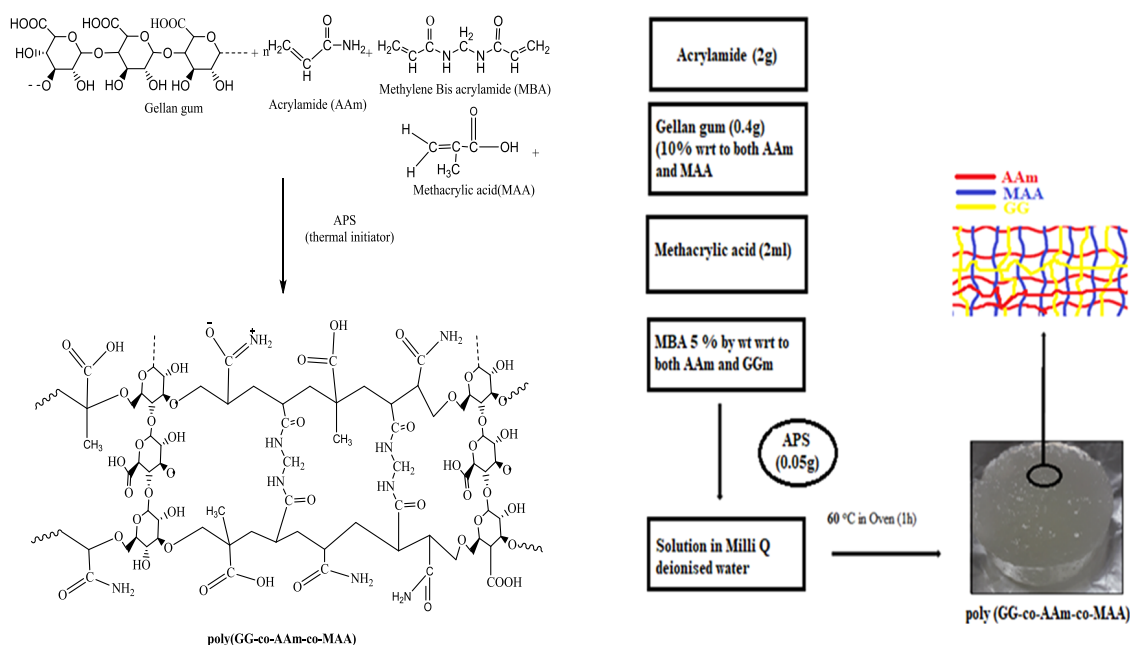
**Revised:** December 28, 2023

**Accepted:** January 12, 2024

**Published:** February 5, 2024



## Scheme 1. Poly(GG-co-AAm-co-MAA) Synthesis and Proposed Mechanism



also affects the immune system, causes itching, watery eyes, and sneezing.<sup>15</sup> Among these dyes, Fuchsin basic (FB), known as Basic Violet 14, and methyl violet (MV) (triphenylmethane) dyes are employed for coloring textiles, silk, leather, paper, printing, and plastics. FB dye possesses anesthetic, bactericidal, and fungicidal properties as well. Unfortunately, its discharge into water bodies causes severe environmental concerns and has adverse effects on human health, including quadriplegia, elevated heart rate, tissue necrosis, and jaundice and can cause cancer due to its toxicity and nonbiodegradability.<sup>16,17</sup> Due to such a harmful effect, dye removal is imperative from aqueous solution. For the removal of FB dye, Ibrahim et al. used a hydrogel synthesized from acrylamide/sodium methacrylate/chitosan,<sup>18</sup> and Sayed et al. used a hydrogel made of gum-poly(vinylpyrrolidone)-*co*-silica nanocomposite materials. Similarly, for the removal of methyl violet, Mittal et al. used a graphene oxide cross-linked hydrogel and Rehman et al. use zwitterionic polymeric hydrogels.<sup>19</sup> Several wastewater techniques like photocatalytic degradation,<sup>20</sup> electrochemical degradation,<sup>21</sup> and adsorption<sup>22</sup> are in use for the elimination of dyes. Among these techniques, adsorption is superior from the mentioned ones along flocculation, filtration, precipitation, and chemical coagulation methods, owing to the high stability, flexibility, low cost, excellent performance, and ease of operation in dye removal from water.<sup>23</sup> Various adsorbents like rice husk,<sup>24</sup> activated carbon,<sup>25</sup> and biomass<sup>26</sup> have been used for the removal of dyes.

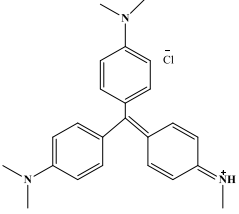
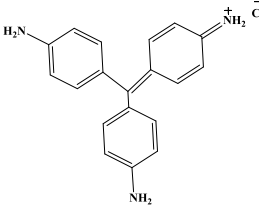
Recently, polymeric materials, like hydrogels, have gained attention as effective adsorbents for dye removal. They are unique because of their simple processing, ease of regeneration, and ability to be molded into various shapes, such as beads, sheets, and membranes.<sup>8,27</sup> As the surface chemistry of the adsorbent plays a crucial role in adsorption, copolymerization can improve the surface chemistry of the hydrogel for the adsorption of the pollutant by increasing the electrostatic attraction between the target pollutant and the adsorb-

ent.<sup>12,28,29</sup> Therefore, in the current study, a pH-sensitive, environmentally friendly, nontoxic, and thermally stable superadsorbent hydrogel, i.e., poly(GG-*co*-AAm-*co*-MAA), has been synthesized using polymeric materials like acrylamide, gellan gum (natural polysaccharides), and methacrylic acid. The prepared hydrogel was utilized for the adsorptive removal of cationic dyes such as methyl violet and fuchsin basic from aqueous solution. As acrylamide has a high swelling ability, methacrylic acid containing the COOH functional group and gellan gum are anionic biopolymeric substances having excellent adsorption capacity of dyes and controllable swelling.<sup>10,30</sup> These properties make them the materials of choice for removal of basic (cationic) dyes from wastewater. Gellan gum/acrylamide/methacrylic acid copolymer, abbreviated as poly(GG-*co*-AAm-*co*-MAA), is a terpolymer hydrogel that is considered a novel material since it has not yet been reported in literature (neither its swelling behavior nor its adsorption capabilities toward any dye have been studied yet). Every investigation carried out here regarding novel hydrogels will add useful information to literature.

## 2. EXPERIMENTAL SECTION

**2.1. Materials/Chemicals.** Methyl violet and fuchsin basic dyes (MV, FB, Sigma-Aldrich), and chemicals like acrylamide (AAM, BDH) and gellan gum (GG) were purchased from Sigma-Aldrich; methacrylic acid (MAA) was from Alfa Aesar; the cross-linker *N,N*-methylene bis-AAm (MBA, BDH) and thermal initiator (APS, (NH<sub>4</sub>)<sub>2</sub>S<sub>2</sub>O<sub>8</sub>), ammonium per sulfate, were also from Sigma-Aldrich. NaNO<sub>3</sub> from Merck, NaOH from BDH, and HNO<sub>3</sub> and HCl from Sigma-Aldrich were used without any further processing. Milli-Q water (resistivity 18.2 MΩ-cm, TOC < 5 ppb, and bacterial count 0.01 CFU/mL), distilled water (resistivity 18 MΩ-cm, TOC 200 ppb), and tap water (conductivity 400 μS/cm, TOC 6 ppm, and bacterial count 520 CFU/mL) were used in the experimental work.

Table 1. Physicochemical Properties of Methyl Violet and Fuchsin Basic Dyes<sup>34,16,33</sup>

Properties of dyes	Methyl violet	Fuchsin basic
Chemical formula		
Molecular formula	C <sub>24</sub> H <sub>28</sub> ClN <sub>3</sub> (λ <sub>max</sub> 588 nm)	C <sub>20</sub> H <sub>20</sub> ClN <sub>3</sub> (λ <sub>max</sub> 550 nm)
and		
Molecular mass	393.96 amu	337.85 amu
Solubility	Soluble in water, ethanol and acetone and insoluble in Xylene	Soluble in water, alcohol and acetone and insoluble in Ether

**2.2. Fabrication of Terpolymer of Poly(gellan gum-co-acrylamide-co-methacrylic acid).** A novel gellan gum-based terpolymer hydrogel named poly(gellan gum-co-acrylamide-co-methacrylic acid), abbreviated as poly(GG-co-AAm-co-MAA), was fabricated in situ via a free radical polymerization process.<sup>34,31</sup> It was prepared by mixing 2 g of acrylamide with 2 mL of methacrylic acid and 0.4 g of gellan gum (10% with respect to both AAm and MAA) in MQ-DW. The solution was homogenized through vertexing and sonication at 25 ± 1 °C. Then, 0.12 g of *N,N*-methylene-bis-acrylamide (5% with respect to the weight of both AAm and GG) and 0.05 g of APS were added to the mixture. To get rid of any oxygen that could influence the process, we performed argon purging. The solution was then kept in an electric oven at 60 ± 1 °C for 60 min to initiate the process of polymerization and gelation. To remove any remaining AAm, MAA, and GG that had not been reacted, the polymer was placed in deionized water for 24 h. This left behind an insoluble poly(GG-co-AAm-co-MAA) hydrogel. The copolymeric hydrogel was then dried in a vacuum oven under a pressure of 0.75 kPa at 40 °C (Scheme 1). The desiccated superadsorbent hydrogel was cut into small pieces and stored until the commencement of the dye adsorption experiments.

**2.3. Characterization and Equipment.** Scanning electron microscopy (SEM) analysis was conducted using a JSM5910 instrument manufactured by JEOL, Tokyo, Japan. Fourier transform infrared spectroscopic (FTIR) study was conducted using the Japanese standard JIS 0208-1990. To determine the optical properties, a double-beam UV/vis spectrophotometer was used; specifically, the UV-1800 model by Shimadzu Scientific Instruments Inc. in Tokyo, Japan, was utilized in the range 200–800 nm. X-ray diffractometry (XRD) was performed utilizing a Panalytical X' Pert 161 Pro instrument (2θ range of 10–80°). Using a TGA 851e instrument made by Mettler Toledo, thermal gravimetric analysis (TGA) was performed. The Brunauer–Emmett–Teller (BET) analysis, specifically employing the

NOVA-2000E instrument, was conducted through nitrogen adsorption–desorption at a temperature of 77.2 K, utilizing a sample mass of 0.0214 g. Pore size distribution was determined using both Barrett–Joyner–Halenda (BJH) and Dubinin–Radushkevich (DR) methods.

**2.4. Swelling Study.** The swelling behavior of the superabsorbent was examined at 298 K using both tap and distilled water (at pH 7). The swelling behavior of the terpolymer was also studied at various pH (pH 4, pH 7, pH 9, pH 11) using the gravimetric method, as previously documented.<sup>28,31</sup> The procedure involved was as follows: taking a precisely weighed dry sample of the hydrogel and immersing it in separate containers with 200 mL of distilled and tap water. The weight of the hydrogel was recorded at specific time intervals, after every 30 min, until a constant weight was achieved. This constancy in weight indicated that the hydrogel had reached equilibrium in terms of swelling. Before the weight was measured, any surface water was carefully removed using tissue paper. The water absorbency was then quantitatively assessed, expressed as % swelling and swelling content, providing valuable insights into the superabsorbent swelling properties, calculated using eq 1.<sup>32</sup>

$$\% \text{ swelling} = \frac{w_s - w_d}{w_d} \times 100 \quad (1)$$

where  $w_s$  is the weight of the enlarged hydrogel and  $w_d$  is the weight of the dry ter-polymer gel.

**2.5. Study of Adsorption (Experiments).** In the batch absorption experiments, poly(GG-co-AAm-co-MAA) hydrogel was employed to remove methyl violet and Fuchsin Basic dyes from aqueous solution. In each study, 0.05 g of a sample of terpolymer was introduced into a 10 mL solution containing dyes. The pH of the solution was adjusted at a pH 7 using NaOH and HNO<sub>3</sub>, and recorded using a pH meter (pH-2601); then, the mixture was agitated at 200 rpm at 298 K for 30–480 min for equilibrium study and agitated up to 60 min at 293, 313, and 333 K for both kinetics and isotherm studies. A

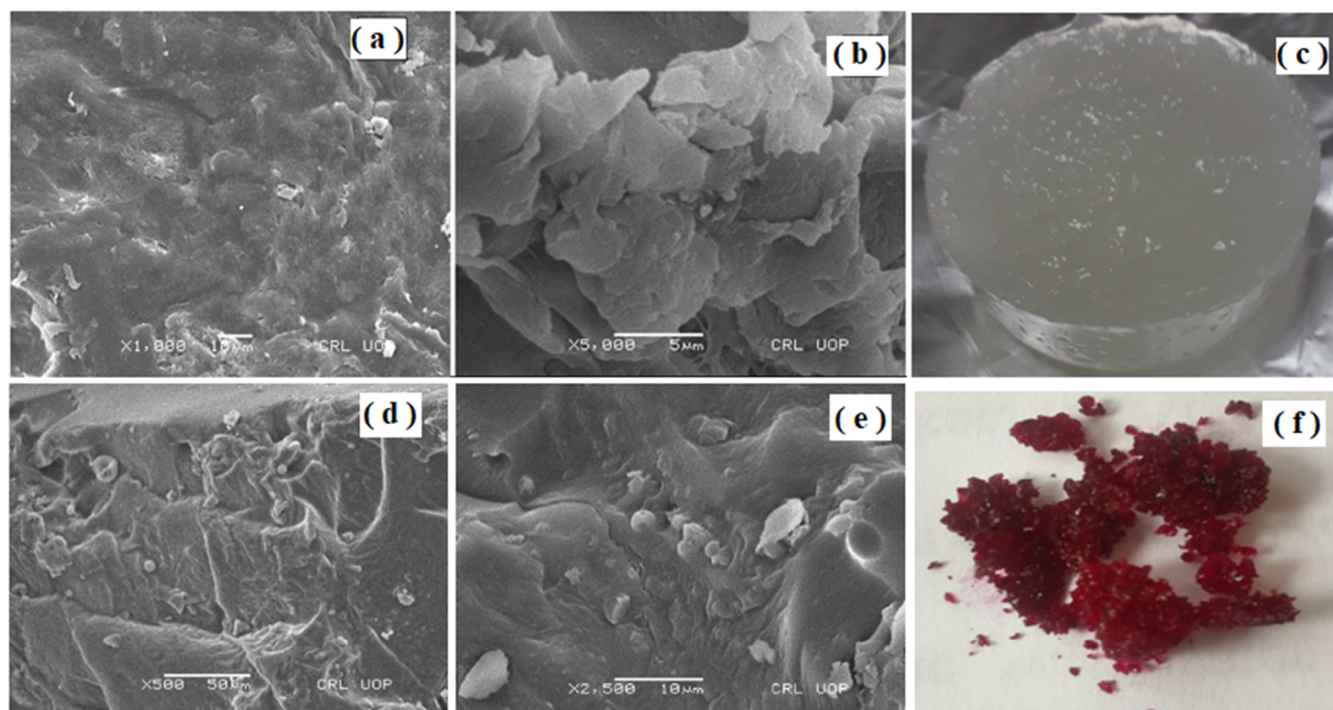


**Figure 1.** SEM of poly(GG-*co*-AAm-*co*-MAA) hydrogel: (a) 10  $\mu\text{m}$ , (b) 5  $\mu\text{m}$ , (c) physical appearance before adsorption, (d) 50  $\mu\text{m}$ , (e) 10  $\mu\text{m}$ , and (f) physical appearance after adsorption. Photographs (c) and (f), courtesy of Shahid Khan. Copyright 2023.

Thermostat Lab Shaker (SH-30) was used for shaking and adjusting temperature. The progress of dye removal was monitored using UV/vis spectroscopy (UV-1800), which measured the absorbance of MV and FB in the solution. The  $\lambda$  max used in this study for MV and FB was 588<sup>34</sup> and 550 nm, respectively. The equilibrium dye concentration was measured by separating the hydrogels from the solution using Whatman-42 filter papers. The kinetics and isotherms were also studied. Table 1 shows the physical properties of the dyes used.<sup>28</sup>

### 3. RESULTS AND DISCUSSION

**3.1. Characterization.** The innovative poly(GG-*co*-AAm-*co*-MAA) hydrogel demonstrated successful synthesis of the hydrogel, as is clear from the SEM images and physical appearance given in Figure 1a–c before adsorption. It shows that the hydrogels have a rough surface and shape. The SEM image reveals the hydrogel is not flat; has an irregular shape with folds and some pores of irregular size and shape due to the grafting of gellan gum with methacrylic acid and acrylamide;<sup>30</sup> and is best suited for the adsorption of dye molecules.<sup>30</sup> The SEM images and physical appearance after dye adsorption in Figure 1d–f show the homogeneous smooth surface for terpolymer hydrogels because of the inhibition of the surface active sites of the polymeric hydrogel by dye molecules. The surface functional groups on the copolymeric poly(GG-*co*-AAm-*co*-MAA) hydrogel were recognized using the FTIR spectra in the range of 500–4000  $\text{cm}^{-1}$ , given in Figure 2a. The strong peak at 3324  $\text{cm}^{-1}$  is caused by the OH group of the gellan gum's glucopyranose ring, and its adjacent broad peak is due to the amide functional group. The medium's peaks at 3186 and 1043  $\text{cm}^{-1}$  depict the NH<sub>2</sub> group and C–O–C bond stretching vibration, respectively. The peak measured at 1412 is the result of COO<sup>−</sup> stretching, and the peak at 1319 is due to the bending vibration of the CONH

amide group. A noticeable band at 1443  $\text{cm}^{-1}$  is owing to the C–N stretching vibration from the link of AAm with the GG. The peaks in the range of 1647 and 1599  $\text{cm}^{-1}$  are due to the C=O amide and COO<sup>−</sup> bond stretching provided, indicating the presence of the amide and MAA. The peaks at 2929  $\text{cm}^{-1}$  are a result of CH<sub>2</sub> bond stretching vibrations. The successful synthesis was confirmed by the broad peak of amide near 3400 nm due to the presence of water molecules as this peak appears sharp in pure acrylamide.<sup>34,31,35</sup> The peaks for both gellan gum and acrylamide present in the spectra of "FTIR" indicate that the p(GG-*co*-AAm-*co*-MAA) hydrogel was really constructed, which can also be confirmed from the physical appearance of the hydrogel after the polymerization. Similar results are shown elsewhere.<sup>35</sup> The XRD analysis of the powder polymer sample was done.<sup>8</sup> The diffractogram in Figure 2b contains two broad peaks between 13 and 18° and 20 and 28° showing the amorphous nature of the newly synthesized hydrogels. The spectra also showed a small and broad peak at 50 °C.<sup>36</sup> The amorphous nature was also reported for the polymer of gellan gum with either AAm or MAA in the literature.<sup>35,37</sup> The TGA thermogram of poly(GG-*co*-AAm-*co*-MAA) is shown in Figure 2c. The TGA showed various stages of mass loss of the hydrogel. The first mass loss occurs up to 100 °C temperature, i.e., about 10% is due to the loss of the present moisture. The second mass loss shown by the thermogram of the synthesized hydrogel is almost 50% of the original mass at about 390 °C, which is due to the thermal degradation of pAAm chains and those organic components that have lesser ignition point, and may also be due to the dehydration of the –COOH functional groups of the hydrogel. The third stage of thermal degradation is after 400 °C, which is due to the more extensive thermal degradation of the hydrogels. The poly(GG-*co*-AAm-*co*-MAA) gives 29% residue mass at 600 °C, which confirms its thermal stability compared to pAAm and other gellan gum-based hydrogels reported in the literature.<sup>38,39</sup> The N<sub>2</sub> adsorption–

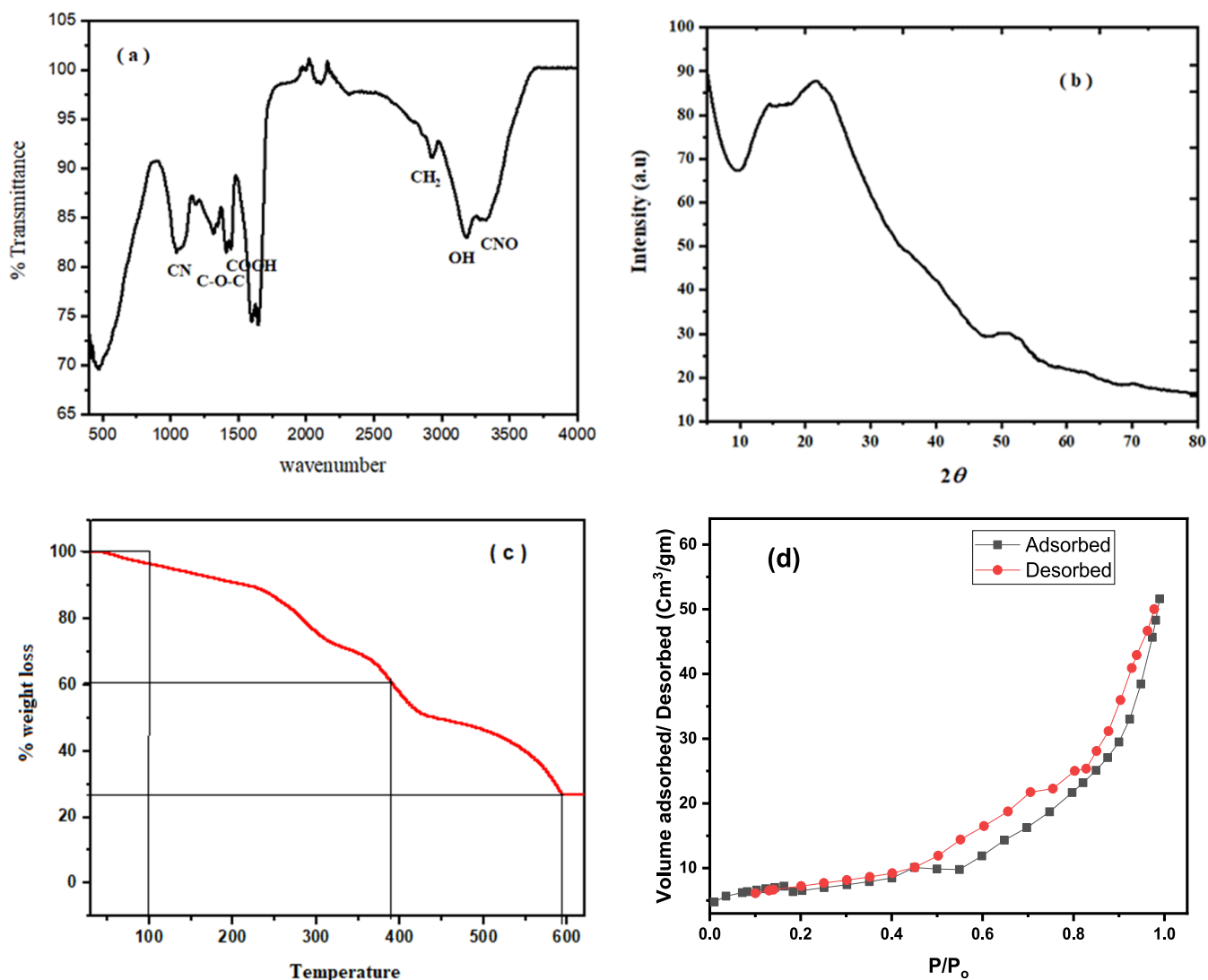


Figure 2. (a) FTIR spectra; (b) XRD spectra; (c) thermogram; (d) BET of the poly(GG-co-AAm-co-MAA) hydrogel sample.

Table 2. BET Surface Area and Pore Size Distribution of the Poly(GG-co-AAm-co-MAA) Hydrogel

surface area (m <sup>2</sup> /g)		pore size distribution					
		BJH methods			DR method		
BET	Langmuir	pore volume (cm <sup>3</sup> /g)	pore diameter (Å)	micropore volume (cm <sup>3</sup> /g)	average pore width (Å)	Ads. energy (kJ/mol)	
19.152 ± 0.0707	22.563	0.05628	9.233	0.0145	9.859	2.033	

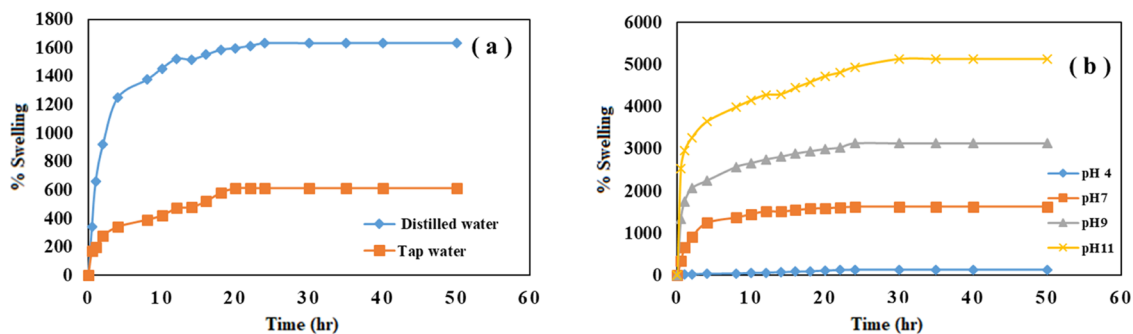
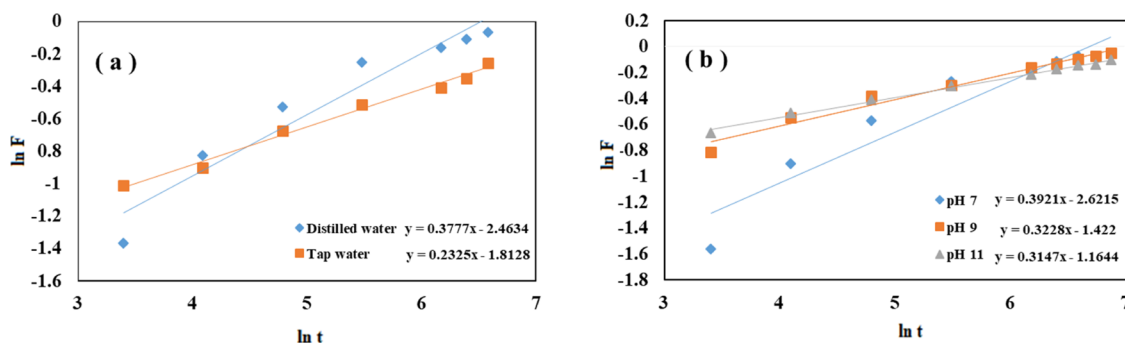


Figure 3. Percent swelling of poly(GG-co-AAm-co-MAA) in (a) distilled water and tap water at neutral pH and (b) poly(GG-co-AAm-co-MAA) at various pH. Conditions: temperature 298 K, pH adjusted by 0.1 M HNO<sub>3</sub> and 0.1 M NaOH, pH range (pH 4, pH 7, pH 9, pH 11).



**Figure 4.**  $\ln t$  vs  $\ln F$  plots for swelling of p(GG-co-AAm-co-MAA): (a) distilled water and tap water at neutral pH and (b) poly(GG-co-AAm-co-MAA) hydrogel at various pH (4–11).

desorption isotherms of poly(GG-co-AAm-co-MAA) are depicted in Figure 2d. The area under the hysteresis loop exhibited an increase with processing temperature, indicating an expanded pore size distribution. The isotherms of the terpolymer displayed a distinctive type-IV curve. Employing the Brunauer–Emmett–Teller (BET) method, the specific surface area of the poly(GG-co-AAm-co-MAA) hydrogel (Table 2) was determined to be 19.152 m<sup>2</sup>/g. Additionally, the BJH and DR methods were employed for pore size calculations, aligning with the values reported for other comparable hydrogels in the literature.<sup>40,41</sup>

**3.2. Swelling Study.** The swelling potential of poly(GG-co-AAm-co-MAA) was inspected thoroughly in distilled and tap water under neutral pH, Figure 3a, and also at various pH (4–11), Figure 3b, in order to find the effect of pH on the swelling behavior of the hydrogels as a function of time. The results show the superabsorptive nature of the synthesized polymeric gel in both distilled and tap water. The poly(GG-co-AAm-co-MAA) superabsorbent hydrogel exhibited rapid water uptake initially followed by a slow decline until the accomplishment of equilibrium at the 22nd hour in distilled water and the 20th hour in tap water. The maximum % water absorptivity corresponding to the equilibrium point was 1633 in distilled water and 612.7% in tap water under neutral (pH = 7) conditions. In the case of the % swelling study at various pH, the % water absorptivity at equilibrium point was 1633% (at pH = 7), 3130% (at pH = 9), and 5132% (at pH = 11). The remarkable % swelling may have stemmed from the predominant electrostatic repulsion between the  $-\text{COO}^-$  groups of gellan gum and MAA.<sup>42</sup> In the case of swelling at 4 pH and below, the hydrogel exists in neutral shrunken form due to intermolecular hydrogen bonding between the polymeric chains of the hydrogels. So, the pores in the hydrogels are closed and the diffusion of water into the hydrogel is difficult and the % swelling decreases.<sup>43</sup>

**3.2.1. Ficks Law and Water Diffusion.** The type of water diffusion into the poly(GG-co-AAm-co-MAA) hydrogels during swelling was studied using Ficks law.<sup>28</sup> The percent swelling was used for calculation of the swelling fraction ( $F$ ) using eq 2 and for  $\ln F$ , eq 3 was used.

$$F = \frac{S_t}{S_0} = kt^n \quad (2)$$

$$\ln F = \ln k + n \ln t \quad (3)$$

The percent swelling is  $S_t$  at time  $t$  and  $S_0$  at equilibrium. The constant  $k$  is the network structure of the hybrid material, and the  $n$  in eq 3 is the diffusion exponential of the solvent. For

the calculation, the slope and intercept of the  $\ln F$  versus  $\ln t$  linear plots given in Figure 4a,b were plotted. The graphs  $\ln F$  versus  $\ln t$  for values of  $n \leq 0.5$  and an  $R^2$  value closer to 1 (0.989) presented in Table 3 for the synthesized poly(GG-co-AAm-co-MAA) hydrogels show Fickian type of water diffusion.<sup>37,28</sup>

**Table 3.** Swelling Properties of Poly(GG-co-AAm-co-MAA) in Distilled Water and Tap Water at Neutral pH and at pH Range of (7–11)

hydrogels	pH 7	$n$	$K$	$R^2$
poly(GG-co-AAm-co-MAA)	distilled water	0.3777	0.0851	0.9327
	tap water	0.2325	0.1632	0.9891
poly(GG-co-AAm-co-MAA)	pH 7	0.3777	0.0852	0.904
	pH 9	0.3228	0.2455	0.9755
	pH 11	0.3147	0.3065	0.9944

**3.3. Absorption Study.** **3.3.1. Effect of pH on Dye Adsorption.** The synthesized poly(GG-co-AAm-co-MAA) hydrogel contains pH-sensitive functionalities like amide ( $\text{CONH}_2$ ) and  $\text{COOH}$ . The variation in pH of the aqueous medium strongly affects the surface charges of the hydrogel, which affects its dye adsorption capacity. The amount of MV and FB dyes adsorbed at various pH values by poly(GG-co-AAm-co-MAA) hydrogel is depicted in Figure 5. The figures show that the adsorption of both the dyes increases when the pH of the solution increases and the maximum adsorption

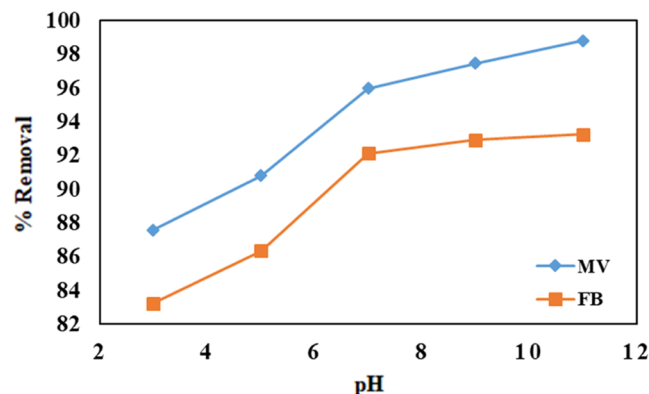


**Figure 5.** Effect of pH on the percent removal of MV and FB dyes by the poly(GG-co-AAm-co-MAA) hydrogel. Conditions: dose 0.05, temperature 298 K, time 8 h, pH range (3–11) adjusted by 0.1 M NaOH and 0.1 M  $\text{HNO}_3$ , and volume used 10 mL.

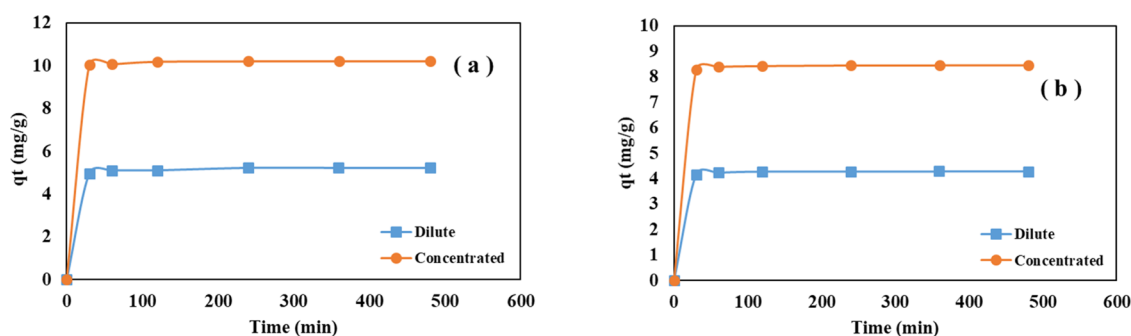
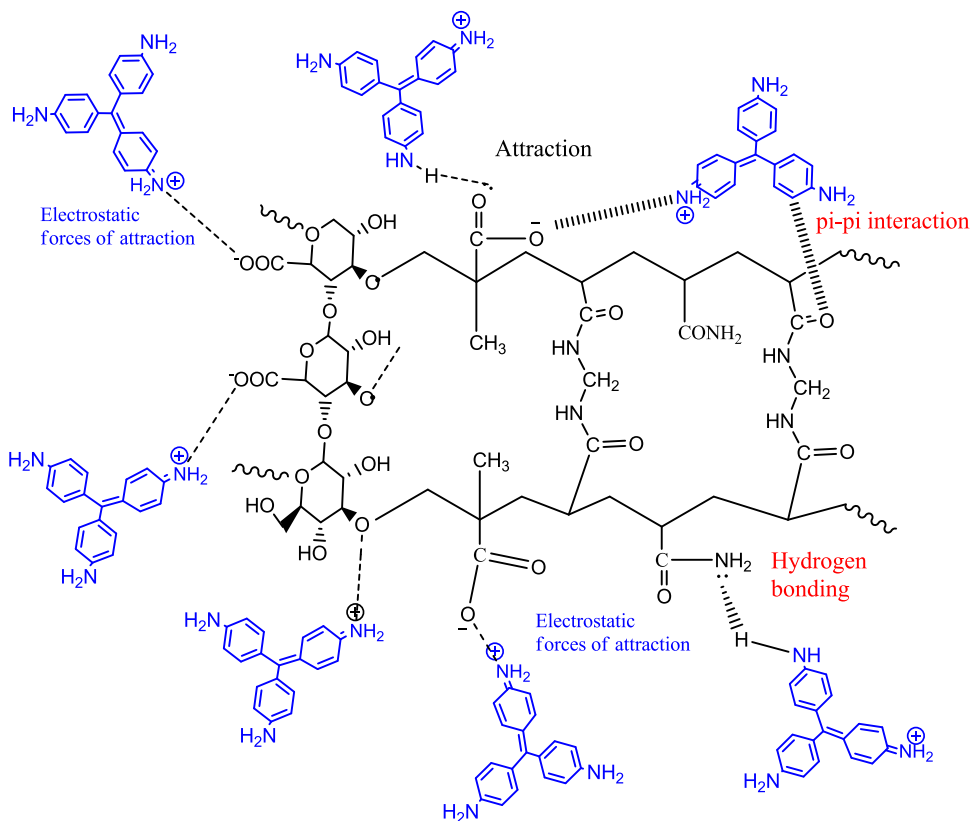


**Figure 6.** Equilibration time for the adsorption of (a) MV and (b) FB by the poly(GG-co-AAm-co-MAA) hydrogel. Conditions: temperature 298 K, dye volume 10 mL, dose 0.05 g, time 8 h, pH 7.

### Scheme 2. Proposed Mechanism for the Adsorption of Dyes (Cationic) on Poly(GG-co-AAm-co-MAA) Hydrogels



occurred at pH 11. The highest sorption potential observed at pH 11 may be attributed to the coexistence of the protonated dye molecule and deprotonated hydrogel COOH functional groups, facilitating electrostatic binding.<sup>44</sup> The percentage of dye elimination is determined by eq 4.<sup>28</sup>

$$\text{percent removal} = \frac{c_i - c_t}{c_i} \times 100 \quad (4)$$

where the initial concentration is  $c_i$ , and  $c_t$  is the equilibrium concentration of the dye used.

**3.3.2. Equilibration Time.** The equilibration study shows the impact of time on the absorption capacity within a contact time (equilibration) range of 30–480 min. Initially, an obvious rise in adsorption capacity was observed over time, followed by a change in adsorption rates. This phenomenon is due to the fact that at the start all active sites of hydrogel were unoccupied and available for dye molecules. However, as time passed, the

active sites on the hydrogel became gradually filled, leaving limited space for further dye adsorption. Consequently, the adsorption of dyes decreases with the passage of time, as illustrated in Figure 6 (a) for MV and (b) for FB. The figures showed 60 min equilibration time for the adsorption of both dyes. Scheme 2 shows the proposed mechanism for the adsorption of cationic dye molecules on the surface of hydrogel.

**3.4. Adsorption Kinetics Study.** The kinetics study for dye adsorption was conducted on the poly(GG-co-AAm-co-MAA) hydrogel to elucidate its adsorption mechanism. 0.05 g of the adsorbent was introduced into two separate flasks containing 10 mL of dye solution ( $7 \times 10^{-5}$  M) of MV and FB. The study was carried out at various temperatures (293, 313, and 333 K) over a specific period of time ranging from 10 to 60 min, using a thermostat shaker bath. The calculated kinetic parameters based on the experimental data at different time intervals provide an understanding of the feasibility of the

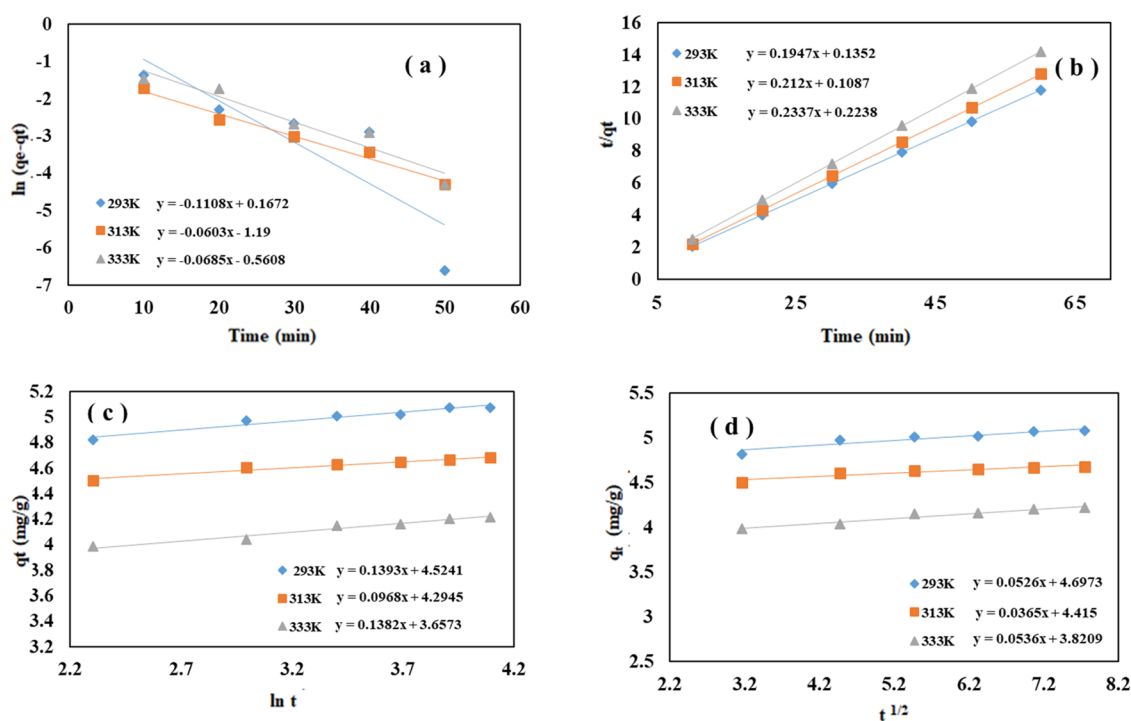


**Figure 7.** Kinetics study for MV adsorption on p(GG-co-AAm-co-MAA) hydrogel: (a) pseudo-first order, (b) pseudo-second order, (c) Elovich model, and (d) intraparticle diffusion. Conditions for the study: dose 0.05 g, volume 10 mL, time 60 min, pH 7, temperature 293, 313, and 333 K.

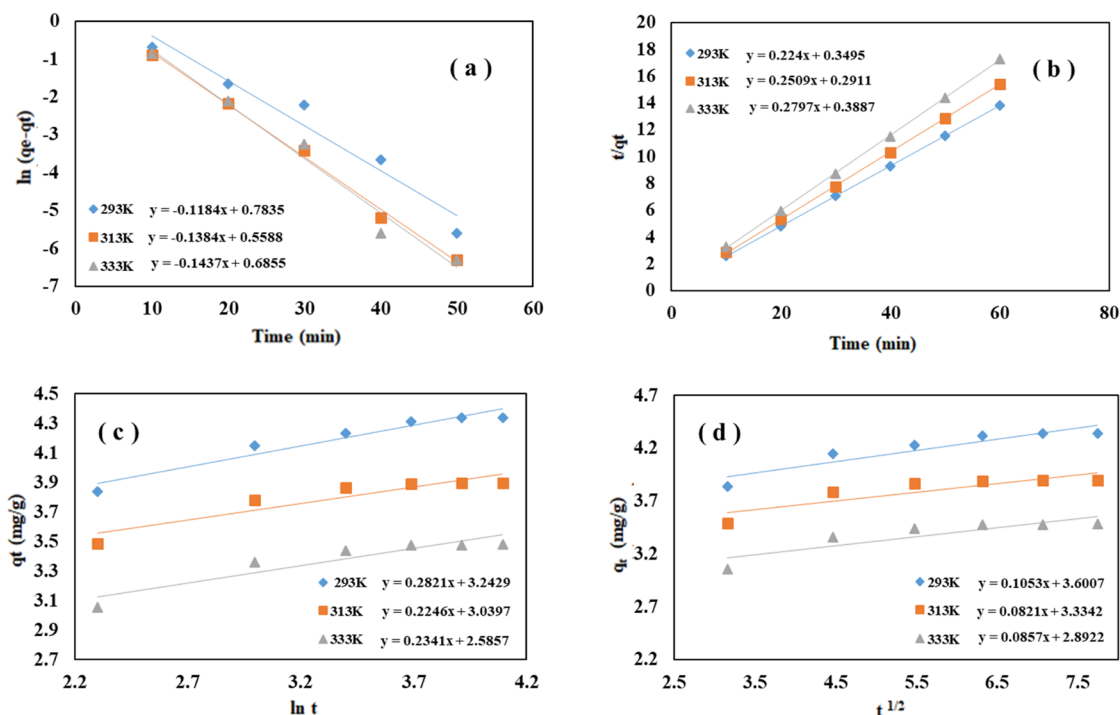


**Figure 8.** Kinetics study for FB adsorption on p(GG-co-AAm-co-MAA) hydrogel: (a) pseudo-first order, (b) pseudo-second order, (c) Elovich model, and (d) intraparticle diffusion. Conditions for the study: dose 0.05 g, volume 10 mL, time 60 min, pH 7, temperature 293, 313, and 333 K.

adsorption process.<sup>45</sup> Four different types of kinetic models were applied to analyze the adsorption kinetics, namely, the pseudo-first order (Figure 7a), pseudo-second order (Figure 7b), Elovich (Figure 7c), and intraparticle diffusion models (Figure 7d) for MV and, similarly, Figure 8a–d for FB using eqs 5–8.<sup>41</sup>

$$\log(q_e - q_t) = \log q_e - \frac{k_1 t}{2.303} \quad (5)$$

$$\frac{t}{q_t} = \frac{t}{q_e} + \frac{1}{k_2 q_e^2} \quad (6)$$

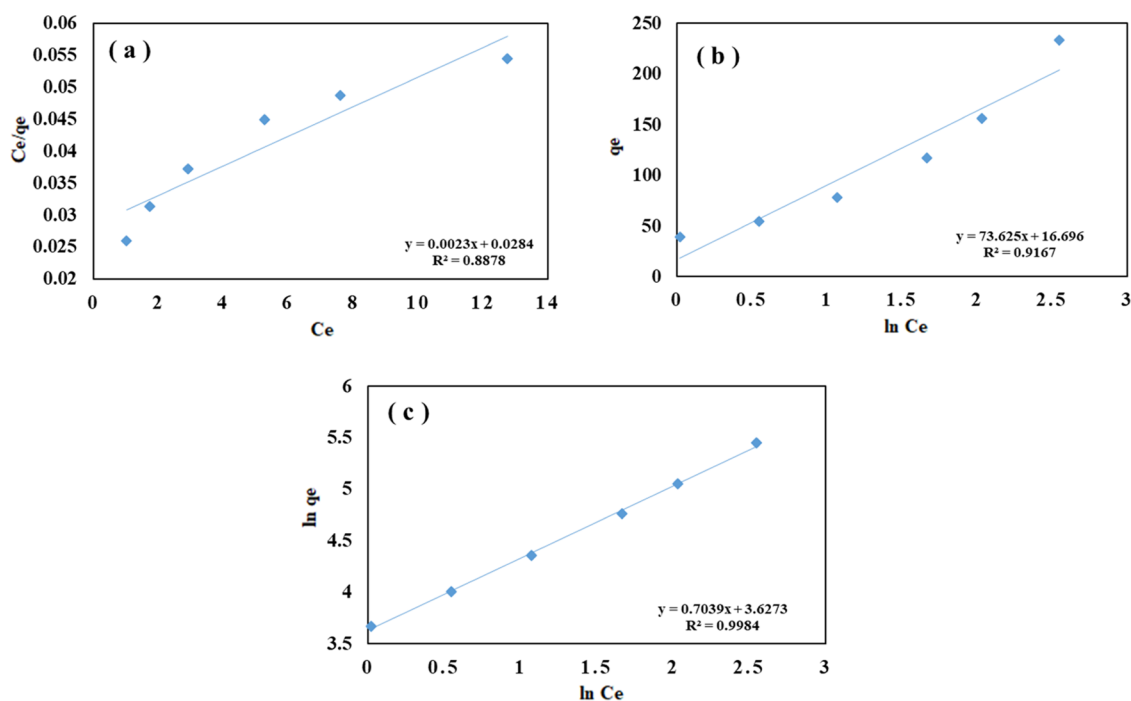


**Table 4.** Calculated Pseudo-First-Order and Pseudo-Second-Order Parameters for the Kinetic Study of MV and FB Dyes Adsorbed on the p(GG-co-AAm-co-MAA) Hydrogel Sample

hydrogels	pseudo-first order					pseudo-second order			
	Temp (K)	$k_1$ (min <sup>-1</sup> )	$q_e$ (mg/g) (cal)	$q_e$ (mg/g) (exp)	$R^2$	$k_2$ (mg/g·min)	$q_e$ (mg/g) (cal)	$q_e$ (mg/g) (exp)	$R^2$
poly(GG-co_AAm-co-MAA) (methyl violet)	293	0.1108	1.181	5.709	0.7598	0.280	5.136	5.709	1
	313	0.0603	0.304	4.682	0.9803	0.413	4.716	4.682	1
	333	0.0685	0.570	4.218	0.9321	0.2442	4.278	4.218	0.999
poly(GG-co_AAm-co-MAA) (Fuchsin Basic)	293	0.1184	2.188	4.340	0.9529	0.143	4.464	4.340	1
	313	0.1384	1.748	3.897	0.9951	0.216	3.985	3.897	0.999
	333	0.1437	1.984	3.479	0.977	0.201	3.575	3.479	0.999

**Table 5.** Elovich Model and Intraparticle Diffusion Models' Calculated Parameters for MV and FB Dyes Adsorbed on the p(GG-co-AAm-co-MAA) Hydrogel Sample

hydrogels	intraparticle diffusion model				Elovich model		
	Temp (K)	$k_{id}$	$C$	$R^2$	$\beta$	$\alpha$	$R^2$
poly(GG-co-AAm-co-MAA) (methyl violet dye)	293	0.0526	4.6973	0.8888	7.178	13.244	0.9464
	313	0.0365	4.415	0.9019	10.33	18.248	0.9616
	333	0.0536	3.8209	0.9534	7.275	10.691	0.9623
poly(GG-co-AAm-co-MAA) (Fuchsin Basic dye)	293	0.1053	3.6007	0.8565	3.544	4.442	0.934
	313	0.0821	3.3342	0.7548	4.452	5.228	0.8572
	333	0.0857	2.8922	0.7595	4.271	4.165	0.861

**Figure 9.** Isotherm model for MV dyes' adsorption on p(GG-co-AAm-co-MAA) hydrogel: (a) Langmuir isotherm, (b) Temkin, and (c) Freundlich isotherm model. Conditions for the study: dose 0.05 g, volume 10 mL, time 60 min, pH 7, and temperature 293 K.

$$q_t = \frac{\ln \beta \alpha}{\alpha} + \frac{\ln t}{\beta} \quad (7)$$

$$q_t = K_{id} t^{1/2} + C \quad (8)$$

These equations involve parameters such as the equilibrium adsorption capacity ( $q_e$ ), adsorption capacity at time  $t$  ( $q_t$ ), pseudo-first-order rate constant ( $k_1$ , 1/min), pseudo-second-order rate constant ( $k_2$ , g/mg·min), initial adsorption rate ( $\alpha$ , mg/g·min), intercept ( $C$ ), desorption constant ( $\beta$ , mg/g·min), and intraparticle diffusion constant ( $k_{id}$ , mg/g·min)<sup>45</sup>. The

results presented in Table 4 reveal that the second-order kinetics model is best fitted to the adsorption data as characterized by an  $R^2$  value closer to 1 and the greater agreement between  $q_e$  calculated and  $q_e$  experimental values.<sup>46</sup> Additionally, the Elovich model was applied to describe dye adsorption on the synthesized hydrogel at various temperatures. The increase in  $\beta$  value (Table 5) with temperature shows that low temperature is the optimum temperature for dye adsorption.<sup>47</sup> Furthermore, the intraparticle diffusion model was employed, displaying a multilinear behavior in the adsorption of dye onto the prepared hydrogel, indicating the

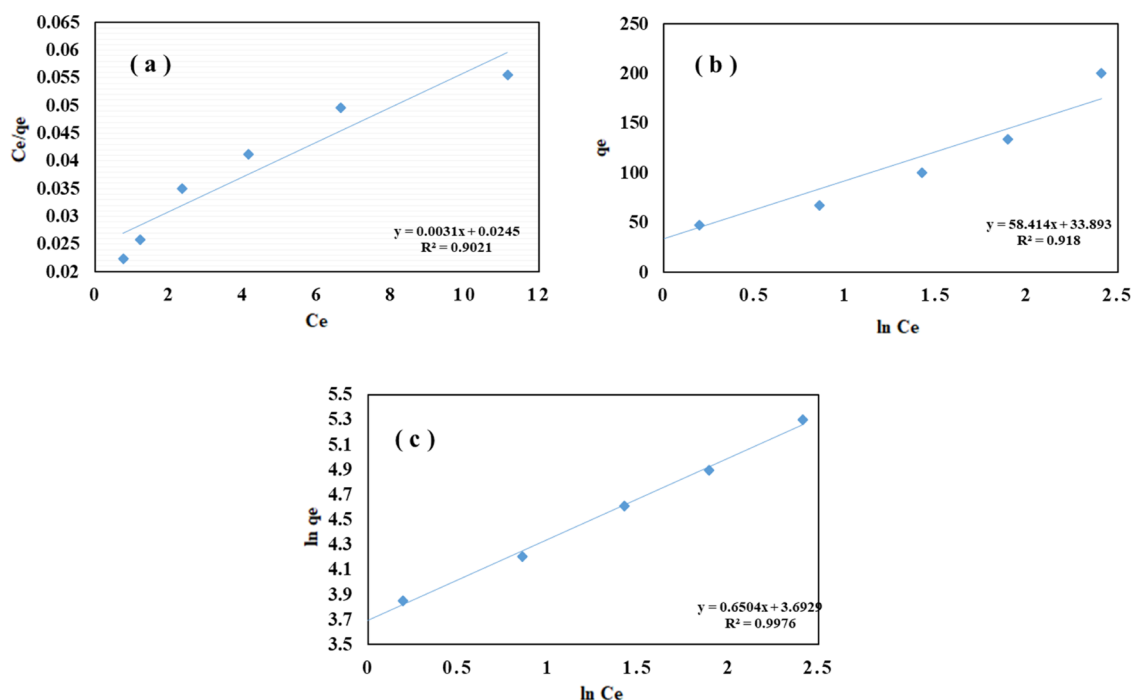


**Figure 10.** Isotherm model for FB dye adsorption on p(GG-co-AAm-co-MAA) hydrogel. (a) Langmuir isotherm, (b) Temkin, and (c) Freundlich isotherm model. Conditions for the study: dose 0.05 g, volume 10 mL, time 60 min, pH 7, and temperature 293 K.

involvement of multiple kinetic steps. The plots presented in Figures 7d and 8d for intraparticle diffusion of both dyes show that the line in the plots does not intersect the origin. This observation serves to confirm that both film diffusion and intraparticle diffusion play a role in constraining the rate of the adsorption process to a certain degree.<sup>48,49</sup> The calculated parameters obtained are summarized in Table 4 for pseudo-first-order and pseudo-second-order and Table 5 for Elovich and intraparticle diffusion models.

**3.5. Isotherm Study.** Various isotherm models like Freundlich, Langmuir, and Temkin isotherms were employed, and their parameters were calculated to evaluate the surface characteristics and attraction of the hydrogels for dye adsorption. These isotherm models provide an understanding about the interactions between the adsorbate and adsorbent and tell us about the adsorption capacities.<sup>41,46</sup> The maximum adsorption capacity calculated was 233 mg/g (98.9%) for MV and 200 mg/g (98.9%) for FB dyes. The Langmuir isotherm model, represented by eq 9, elucidates the sorption process taking place at the hydrogel surface and provides information about monolayer adsorption. Equation 9 is as follows:

$$\frac{C_e}{q_e} = \frac{C_e}{q_m} + \frac{1}{K_L q_m} \quad (9)$$

Here,  $q_e$  denotes the amount of dye adsorbed at equilibrium (mg/g),  $C_e$  is the solution concentration at equilibrium (mg/L),  $K_L$  is the Langmuir constant, and  $q_m$  signifies the maximum adsorption capacity (mg/g).  $K_L$  and  $q_m$  were determined through the Langmuir plot, as shown in Figure 9a for MV and Figure 10a for FB dyes (Table 6). The small value of  $K_L$  for poly(GG-co-AAm-co-MAA) indicates a weak interaction between the hydrogels and dyes. Furthermore, the small values of correlation coefficient  $R^2$  clearly show that the sorption process is not in accord with the Langmuir isotherm

**Table 6. Measured Parameters for the Adsorption of MV and FB on Poly(GG-co-AAm-co-MAA) Hydrogel at 293 K, Determined from Langmuir, Temkin, and Freundlich Adsorption Isotherm Models**

isotherms		methyl violet	Fuchsin Basic
Freundlich	$K_F$ (mg/g)	37.5	40.13
	$1/n$ (L/g)	0.703	0.65
	$n$	1.42	1.53
	$R^2$	0.998	0.997
Langmuir	$q_m$ (mg/g) Exp	233	200
	$q_m$ (mg/g) Cal	434	322
	$K_L$ (L/g)	0.08	0.126
	$R^2$	0.887	0.911
Temkin	$b$ (J/mol/K)	73	85.4
	$K_T$ (mg/g)	1.25	1.486
	$R^2$	0.91	0.918

model. The Temkin adsorption isotherm model linear equation is given in eq 10

$$q_e = B_1 \ln K_T + B_1 \ln C_e \quad (10)$$

where  $K_T$  (mg/g) and  $B_1$  (J/mol/K) are equilibrium binding and adsorption constant, respectively.<sup>50</sup> The plots,  $q_e$  versus  $\ln C_e$ , give the Temkin isotherm graph: Figure 9b for MV and Figure 10b for FB. The intercept and slope obtained from the  $q_e$  versus  $\ln C_e$  graph were used for the calculation of  $K_T$  given in Table 6 for both the dyes. The small values of  $K_T$  and  $R^2$  for dye adsorption on the poly(GG-co-AAm-co-MAA) hydrogel show the weak interaction between the hydrogels and dyes, which evidently indicates that the sorption process is not according to the Temkin isotherm model. Therefore, the Freundlich model, expressed in eq 11, was employed to assess the adsorption reversibility, nonideal behavior, and multilayer adsorption of dye molecules on the surface of the hydrogel using eq 11

$$\ln q_e = \ln K_F + \frac{1}{n} \ln C_e \quad (11)$$

In this equation,  $q_e$  represents the amount of adsorbed dye at equilibrium,  $C_e$  is the equilibrium dye concentration,  $K_F$  stands for the capacity of adsorption, and  $1/n$  is the intensity of adsorption; the  $1/n$  value provides information about the adsorption nature and feasibility. If the value of  $1/n$  is between 0 and 1, it indicates favorable adsorption, and a value greater than 1 indicates unfavorable adsorption.<sup>51</sup> The calculated parameters were obtained from the intercept and slope values of the graph plotted between  $\ln q_e$  and  $\ln C_e$  as depicted in Figure 9c for MV and Figure 10c for FB dyes. In this study, the value of  $1/n$  is less than 1, i.e., 0.703 for MV and 0.65 for FB (Table 6). Moreover, the comparison of the Freundlich constant ( $K_F$ ), Temkin constant ( $K_T$ ), and Langmuir constant ( $K_L$ ) signifies that the Freundlich isotherm model is the best fitted model for elucidating the adsorption of MV and FB on poly(GG-co-AAm-co-MAA) hydrogel.

**3.6. Thermodynamic Study.** Thermodynamic study was done at various temperatures (293, 313, and 333 K) by calculating  $\Delta S^\circ$  (entropy change),  $\Delta G^\circ$  (Gibbs free energy change), and  $\Delta H^\circ$  (enthalpy change), using Vont Hoff's eqs 12–14.<sup>31,52</sup>

$$\Delta G^\circ = -RT \ln K \quad (12)$$

$$\ln K = \frac{\Delta S^\circ}{R} - \frac{\Delta H^\circ}{RT} \quad (13)$$

$$\Delta G^\circ = \Delta H^\circ - T\Delta S^\circ \quad (14)$$

The  $T$  in the equation represents the temperature in kelvin,  $R$  (8.314 kJ/mol/K) is the gas constant (universal), and  $K$  is the thermodynamic equilibrium constant calculated from  $q_e/C_e$ .  $\Delta G$  (J/mol),  $\Delta H$  (J/mol), and  $\Delta S$  (J/mol/K) are the changes in Gibbs free energy, enthalpy, and entropy, respectively. The studied parameters are given in Table 7 for

**Table 7. Thermodynamic Parameters for the Removal of MV and FB Dyes by Poly(GG-co-AAm-co-MAA) Hydrogels**

parameters	methyl violet	Fuchsin Basic
$\Delta S^\circ$ (J/mol/K)	−6.07088	−2.42769
$\Delta H^\circ$ (kJ/mol)	−8.82199	−7.83262
$\Delta G^\circ$ (kJ/mol)	293 K	−7.08588
	313 K	−6.82563
	333 K	−6.85538
		−7.03995
		−7.25224
		−6.91934

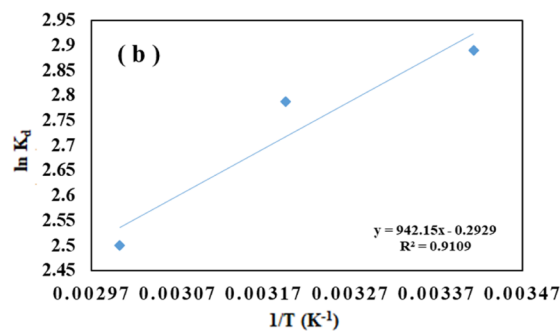
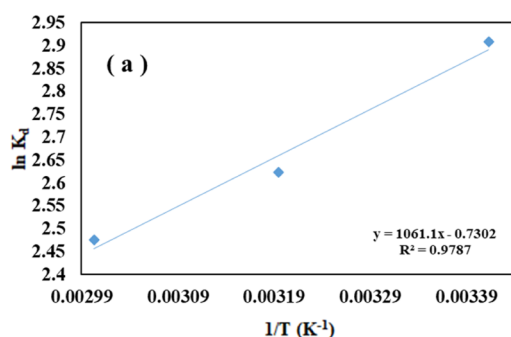


**Figure 11.** Temperature effect on the absorption of (a) MV and (b) FB by poly(GG-co-AAm-co-MAA) hydrogels. Conditions: pH 7, dose 0.05 g, temperature 293, 313, and 333 K.

$\Delta H^\circ$ ,  $\Delta S^\circ$ , and  $\Delta G^\circ$  calculated from the plot of  $1/T$  versus  $\ln k_d$  given in Figure 11a for MV and Figure 11b for FB dyes. The negative  $\Delta H^\circ$  indicates that the adsorption process of MV and FB dyes onto the poly(GG-co-AAm-co-MAA) hydrogel is exothermic; similarly, the negative  $\Delta S^\circ$  suggests that the synthesized hydrogel exhibits an affinity for dyes, leading to reduced randomness at the solid–solution interface during the adsorption process. The negative  $\Delta G^\circ$  value indicates the spontaneous nature of adsorption; moreover, the increase in  $\Delta G^\circ$  with an increase in temperature indicates that lower temperatures favor the adsorption process. The results show that the adsorption is feasible within the experimental temperature range of this study.

**3.7. Regeneration of Poly(GG-co-AAm-co-MAA) Hydrogel for Reuse.** The regenerating experiment was used to find the effectiveness of the synthesized hydrogel as adsorbent for the elimination of MV and FB dyes from wastewater for long period of time. In this experiment, the adsorbed dye molecules within the hydrogel network was extracted using acetone through a solvent extraction method.<sup>31</sup> After treating with acetone and subsequent washing with distilled water for removing any residual solvent or dye, the hydrogel was renewed and made ready for further dye adsorption. As illustrated in Figure 12, the adsorbent was subjected to five

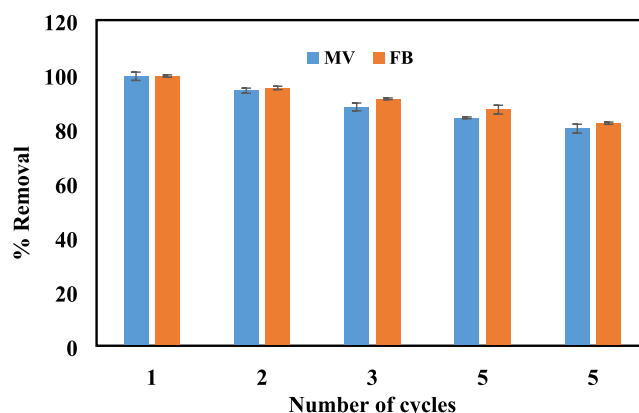


**Figure 12.** Regeneration of the poly(GG-co-AAm-co-MAA) hydrogel for reuse of MV and FB dye removal.

consecutive adsorption desorption cycles, and at the end of the fifth cycle, it still retained more than 82% of its initial efficiency for FB dye and 80% for MV dye removal.

## 4. CONCLUSIONS

Poly(gellan gum-co-acrylamide-co-methacrylic acid) hydrogel was synthesized by the free radical polymerization method. The hydrogel was synthesized from the biopolymers gellan gum (GG), methacrylic acid (MAA), and acrylamide (AAm). MBA was used as the cross-linking agent and APS as the thermal initiator. The hydrogels were characterized using SEM, FTIR, XRD, BET, and TGA techniques. SEM analysis showed a rough surface with pores of various shapes and sizes. FTIR confirmed the presence of amide, methacrylic acid, and gellan gum as is clear from the respective functional groups in the spectra. XRD analysis showed the amorphous nature and TGA confirmed the thermal stability of the synthesized hydrogel. The effects of temperature, pH, contact time, and concentration were also studied and 60 min equilibration time was found. Various isotherms and kinetic models were applied to the experimental data and pseudo-second-order and Freundlich isotherm models were found best fitted for the process. The swelling behavior was studied in tap and distilled water at neutral pH and also in the pH range from 4 to 11. The percent swelling of the hydrogel was 1633% in distilled water, 612.7 in tap water at neutral pH, and 5132 at pH 11. The water diffusion was found to be of Fickian type with  $n \leq 5$ . The enthalpy, Gibbs free energy, and entropy of adsorption showed that the adsorption was an exothermic, spontaneous, and entropy-decreasing process. The maximum capacity of adsorption for MV was 233 mg/g and FB was 200 mg/g. Percent swelling and adsorption capacity increased with the increase in pH of the solution. The hydrogel was successfully regenerated using acetone with more than 80% removal efficiency after the fifth cycle.

## AUTHOR INFORMATION

### Corresponding Author

Muhammad Zahoor – Department of Biochemistry, University of Malakand, Chakdara Dir Lower, KPK 18800, Pakistan; Department of Biochemistry, University of Malakand, Chakdara Dir Lower, KPK 18800, Pakistan; [orcid.org/0000-0002-4528-8517](https://orcid.org/0000-0002-4528-8517); Email: mohammadzahoorus@yahoo.com

### Authors

Shahid Khan – Department of Biochemistry, University of Malakand, Chakdara Dir Lower, KPK 18800, Pakistan; Department of Biochemistry, University of Malakand, Chakdara Dir Lower, KPK 18800, Pakistan  
Najeeb Ur Rahman – Department of Biochemistry, University of Malakand, Chakdara Dir Lower, KPK 18800, Pakistan; Department of Biochemistry, University of Malakand, Chakdara Dir Lower, KPK 18800, Pakistan  
Sultan Alam – Department of Biochemistry, University of Malakand, Chakdara Dir Lower, KPK 18800, Pakistan; Department of Biochemistry, University of Malakand, Chakdara Dir Lower, KPK 18800, Pakistan  
Luqman Ali Shah – National Center of Excellence in Physical Chemistry (NCE), University of Peshawar, Nowshera 25120, Pakistan; [orcid.org/0000-0002-7578-2663](https://orcid.org/0000-0002-7578-2663)  
Muhammad Naveed Umar – Department of Chemistry, University of Liverpool, Liverpool L69 3BX, U.K.  
Riaz Ullah – Department of Pharmacognosy, College of Pharmacy, King Saud University, Riyadh 11451, Saudi Arabia; [orcid.org/0000-0002-2860-467X](https://orcid.org/0000-0002-2860-467X)

Complete contact information is available at:  
<https://pubs.acs.org/10.1021/acsomega.3c07118>

## Notes

The authors declare no competing financial interest.

## ACKNOWLEDGMENTS

The authors extend their appreciation to the researchers supporting Project Number RSP2024R110, and King Saud University, Riyadh, Saudi Arabia, for financial support.

## REFERENCES

- (1) Fujioka, R.; Tanaka, Y.; Yoshimura, T. Synthesis and Properties of Superabsorbent Hydrogels Based on Guar Gum and Succinic Anhydride. *J. Appl. Polym. Sci.* **2009**, *114* (1), 612–616.
- (2) Sharma, K.; Kumar, V.; Kaith, B. S.; Som, S.; Kumar, V.; Pandey, A.; Kalia, S.; Swart, H. C. Synthesis of Biodegradable Gum Ghatti Based Poly (Methacrylic Acid-Aniline) Conducting IPN Hydrogel for Controlled Release of Amoxicillin Trihydrate. *Ind. Eng. Chem. Res.* **2015**, *54* (7), 1982–1991.
- (3) Savina, I. N.; Ingavle, G. C.; Cundy, A. B.; Mikhailovsky, S. V. A Simple Method for the Production of Large Volume 3D Macroporous Hydrogels for Advanced Biotechnological, Medical and Environmental Applications. *Sci. Rep.* **2016**, *6* (1), No. 21154.
- (4) Sharma, K.; Kumar, V.; Swart-Pistor, C.; Chaudhary, B.; Swart, H. C. Synthesis, Characterization, and Anti-Microbial Activity of Superabsorbents Based on Agar–Poly (Methacrylic Acid-Glycine). *J. Bioact. Compat. Polym.* **2017**, *32* (1), 74–91.
- (5) Makhado, E.; Pandey, S.; Ramontja, J. Microwave Assisted Synthesis of Xanthan Gum-Cl-Poly (Acrylic Acid) Based-Reduced Graphene Oxide Hydrogel Composite for Adsorption of Methylene Blue and Methyl Violet from Aqueous Solution. *Int. J. Biol. Macromol.* **2018**, *119*, 255–269.
- (6) Tako, M. The Principle of Polysaccharide Gels. *Adv. Biosci. Biotechnol.* **2015**, *06* (01), 22–36.
- (7) Zheng, M.; Lian, F.; Xiong, Y.; Liu, B.; Zhu, Y.; Miao, S.; Zhang, L.; Zheng, B. The Synthesis and Characterization of a Xanthan Gum-Acrylamide-Trimethylolpropane Triglycidyl Ether Hydrogel. *Food Chem.* **2019**, *272*, 574–579.
- (8) Arun Krishna, K.; Vishalakshi, B. Gellan Gum-based Novel Composite Hydrogel: Evaluation as Adsorbent for Cationic Dyes. *J. Appl. Polym. Sci.* **2017**, *134* (47), No. 45527.
- (9) Wang, F.; Wen, Y.; Bai, T. Thermal Behavior of Polyvinyl Alcohol–Gellan Gum–Al<sup>3+</sup> Composite Hydrogels with Improved Network Structure and Mechanical Property. *J. Therm. Anal. Calorim.* **2017**, *127*, 2447–2457.
- (10) Karthika, J. S.; Vishalakshi, B. Novel Stimuli Responsive Gellan Gum-Graft-Poly (DMAEMA) Hydrogel as Adsorbent for Anionic Dye. *Int. J. Biol. Macromol.* **2015**, *81*, 648–655.
- (11) Rajkumar, D.; Kim, J. G. Oxidation of Various Reactive Dyes with in Situ Electro-Generated Active Chlorine for Textile Dyeing Industry Wastewater Treatment. *J. Hazard. Mater.* **2006**, *136* (2), 203–212.
- (12) Mahapatra, N. N. *Textile Dyes*; CRC Press, 2016.
- (13) Mohammad, A. H. Global Environmental Issues. Hussain, C. M., Ed. In *Handbook of Environmental Materials Management*; Springer, Cham., 2018. DOI: 10.1007/978-3-319-58538-3\_127-1
- (14) Larry, W. World Water Day. A billion people Worldw. lack safe Drink. **2006**.
- (15) Hassaan, M. A. Advanced Oxidation Processes of Some Organic Pollutants in Fresh and Seawater. Ph.D. Thesis, Faculty of Science, Port Said University, 2016.
- (16) Khan, T. A.; Khan, E. A.; Shahjahan. Removal of Basic Dyes from Aqueous Solution by Adsorption onto Binary Iron-Manganese Oxide Coated Kaolinite: Non-Linear Isotherm and Kinetics Modeling. *Appl. Clay Sci.* **2015**, *107*, 70–77.

- (17) Soniya, M.; Muthuraman, G. Recovery of Methylene Blue from Aqueous Solution by Liquid–Liquid Extraction. *Desalin. Water Treat.* **2015**, *53* (9), 2501–2509.
- (18) Ibrahim, A. G.; Sayed, A. Z.; Abd El-Wahab, H.; Sayah, M. M. Synthesis of a Hydrogel by Grafting of Acrylamide-Co-Sodium Methacrylate onto Chitosan for Effective Adsorption of Fuchsin Basic Dye. *Int. J. Biol. Macromol.* **2020**, *159*, 422–432.
- (19) Mittal, H.; Al Alili, A.; Morajkar, P. P.; Alhassan, S. M. Crosslinked hydrogels of polyethylenimine and graphene oxide to treat Cr(VI) contaminated wastewater. *Colloids Surf., A* **2021**, *630*, 127533.
- (20) Cabir, B.; Yurderi, M.; Caner, N.; Agirtas, M. S.; Zahmakiran, M.; Kaya, M. Methylene Blue Photocatalytic Degradation under Visible Light Irradiation on Copper Phthalocyanine-Sensitized TiO<sub>2</sub> Nanopowders. *Mater. Sci. Eng., B* **2017**, *224*, 9–17.
- (21) Saaidia, S.; Delimi, R.; Benredjem, Z.; Mehellou, A.; Djemel, A.; Barbari, K. Use of a PbO<sub>2</sub> Electrode of a Lead-Acid Battery for the Electrochemical Degradation of Methylene Blue. *Sep. Sci. Technol.* **2017**, *52* (9), 1602–1614.
- (22) Ma, P.; Wang, S.; Wang, T.; Wu, J.; Xing, X.; Zhang, X. Effect of Bifunctional Acid on the Porosity Improvement of Biomass-Derived Activated Carbon for Methylene Blue Adsorption. *Environ. Sci. Pollut. Res.* **2019**, *26*, 30119–30129.
- (23) Ince, M.; Ince, O. K. An Overview of Adsorption Technique for Heavy Metal Removal from Water/Wastewater: A Critical Review. *Int. J. Pure Appl. Sci.* **2017**, *3* (2), 10–19.
- (24) Abdelwahab, O.; El Nemr, A.; El Sikaily, A.; Khaled, A. Use of Rice Husk for Adsorption of Direct Dyes from Aqueous Solution: A Case Study of Direct F. Scarlet. *Egypt. J. Aquat. Res.* **2005**, *31* (1), 1–11.
- (25) Malik, P. K. Use of Activated Carbons Prepared from Sawdust and Rice-Husk for Adsorption of Acid Dyes: A Case Study of Acid Yellow 36. *Dyes Pigm.* **2003**, *56* (3), 239–249.
- (26) Laszlo, J. A. Removing Acid Dyes from Textile Wastewater Using Biomass for Decolorization. *Am. Dyest. Rep.* **1994**, *83* (8), 5.
- (27) Matricardi, P.; Cencetti, C.; Ria, R.; Alhaique, F.; Coviello, T. Preparation and Characterization of Novel Gellan Gum Hydrogels Suitable for Modified Drug Release. *Molecules* **2009**, *14* (9), 3376–3391.
- (28) Subhan, H.; Alam, S.; Shah, L. A.; Khattak, N. S.; Zekker, I. Sodium Alginate Grafted Hydrogel for Adsorption of Methylene Green and Use of the Waste as an Adsorbent for the Separation of Emulsified Oil. *J. Water Process Eng.* **2022**, *46*, No. 102546.
- (29) Khan, S. A.; Faizan, S.; Shah, L. A.; Bakhtawara; Zekker, I. Nature of Cross-Linking Matters for the Conditional Removal of CV from Wastewater by Interpenetrating Network Hydrogels. *Int. J. Environ. Sci. Technol.* **2023**, *20* (6), 6723–6734.
- (30) Sharma, K.; Kumar, V.; Kaith, B. S.; Kumar, V.; Som, S.; Kalia, S.; Swart, H. C. Synthesis, Characterization and Water Retention Study of Biodegradable Gum Ghatti-Poly (Acrylic Acid–Aniline) Hydrogels. *Polym. Degrad. Stab.* **2015**, *111*, 20–31.
- (31) Rehman, T. U.; Bibi, S.; Khan, M.; Ali, I.; Shah, L. A.; Khan, A.; Ateeq, M. Fabrication of Stable Superabsorbent Hydrogels for Successful Removal of Crystal Violet from Waste Water. *RSC Adv.* **2019**, *9* (68), 40051–40061.
- (32) Sheikh, N.; Jalili, L.; Anvari, F. A Study on the Swelling Behavior of Poly (Acrylic Acid) Hydrogels Obtained by Electron Beam Crosslinking. *Radiat. Phys. Chem.* **2010**, *79* (6), 735–739.
- (33) Pal, J.; Deb, M. K.; Deshmukh, D. K.; Sen, B. K. Microwave-Assisted Synthesis of Platinum Nanoparticles and Their Catalytic Degradation of Methyl Violet in Aqueous Solution. *Appl. Nanosci.* **2014**, *4*, 61–65.
- (34) Rehman, T. U.; Shah, L. A.; Khan, M.; Irfan, M.; Khattak, N. S. Zwitterionic Superabsorbent Polymer Hydrogels for Efficient and Selective Removal of Organic Dyes. *RSC Adv.* **2019**, *9* (32), 18565–18577.
- (35) Zheng, M.; Cai, K.; Chen, M.; Zhu, Y.; Zhang, L.; Zheng, B. PH-Responsive Poly (Gellan Gum-Co-Acrylamide-Co-Acrylic Acid) Hydrogel: Synthesis, and Its Application for Organic Dye Removal. *Int. J. Biol. Macromol.* **2020**, *153*, 573–582.
- (36) Sharma, K.; Kaith, B. S.; Kumar, V.; Kalia, S.; Kumar, V.; Som, S.; Swart, H. C. Gum Ghatti Based Novel Electrically Conductive Biomaterials: A Study of Conductivity and Surface Morphology. *eXPRESS Polym. Lett.* **2014**, *8* (4), 267.
- (37) Kim, B.; La Flamme, K.; Peppas, N. A. Dynamic Swelling Behavior of PH-sensitive Anionic Hydrogels Used for Protein Delivery. *J. Appl. Polym. Sci.* **2003**, *89* (6), 1606–1613.
- (38) Şolpan, D.; Torun, M.; Güven, O. The Usability of (Sodium Alginate/Acrylamide) Semi-interpenetrating Polymer Networks on Removal of Some Textile Dyes. *J. Appl. Polym. Sci.* **2008**, *108* (6), 3787–3795.
- (39) Thomas, L. C. Use of Multiple Heating Rate DSC and Modulated Temperature DSC to Detect and Analyze Temperature-Time-Dependent Transitions in Materials. *Am. Lab.* **2001**, *33* (1), 26–31.
- (40) Safavi-Mirmahalleh, S.-A.; Salami-Kalajahi, M.; Roghani-Mamaqani, H. Effect of Surface Chemistry and Content of Nanocrystalline Cellulose on Removal of Methylene Blue from Wastewater by Poly (Acrylic Acid)/Nanocrystalline Cellulose Nanocomposite Hydrogels. *Cellulose* **2019**, *26*, 5603–5619.
- (41) Jabeen, S.; Alam, S.; Shah, L. A.; Ullah, M. Successful Preparation of Tercopolymer Hydrogel for the Removal of Toluidine Dye from Contaminated Water: Experimental and DFT Study. *Sep. Sci. Technol.* **2023**, *58*, 1923–1938.
- (42) Yuan, Z.; Wang, J.; Wang, Y.; Liu, Q.; Zhong, Y.; Wang, Y.; Li, L.; Lincoln, S. F.; Guo, X. Preparation of a Poly (Acrylic Acid) Based Hydrogel with Fast Adsorption Rate and High Adsorption Capacity for the Removal of Cationic Dyes. *RSC Adv.* **2019**, *9* (37), 21075–21085.
- (43) Subhan, H.; Alam, S.; Shah, L. A.; Ali, M. W.; Farooq, M. Sodium Alginate Grafted Poly (N-Vinyl Formamide-Co-Acrylic Acid)-Bentonite Clay Hybrid Hydrogel for Sorptive Removal of Methylene Green from Wastewater. *Colloids Surf., A* **2021**, *611*, No. 125853.
- (44) Zia, K. M.; Tabasum, S.; Khan, M. F.; Akram, N.; Akhter, N.; Noreen, A.; Zuber, M. Recent Trends on Gellan Gum Blends with Natural and Synthetic Polymers: A Review. *Int. J. Biol. Macromol.* **2018**, *109*, 1068–1087.
- (45) El-Bindary, M. A.; El-Deen, I. M.; Shoaib, A. F. Removal of Anionic Dye from Aqueous Solution Using Magnetic Sodium Alginate Beads. *J. Mater. Environ. Sci.* **2019**, *10* (7), 604–617.
- (46) Thue, P. S.; Lima, D. R.; Naushad, M.; Lima, E. C.; de Albuquerque, Y. R. T.; Dias, S. L. P.; Cunha, M. R.; Dotto, G. L.; de Brum, I. A. S. High Removal of Emerging Contaminants from Wastewater by Activated Carbons Derived from the Shell of Cashew of Para. *Carbon Lett.* **2021**, *31*, 13–28.
- (47) Chrzan, M.; Chlebda, D.; Jodłowski, P.; Salomon, E.; Kołodziej, A.; Gancarczyk, A.; Sitarz, M.; Łojewska, J. Towards Methane Combustion Mechanism on Metal Oxides Supported Catalysts: Ceria Supported Palladium Catalysts. *Top. Catal.* **2019**, *62*, 403–412.
- (48) Özacar, M.; Şengil, I. A. Application of Kinetic Models to the Sorption of Disperse Dyes onto Alunite. *Colloids Surf., A* **2004**, *242* (1–3), 105–113.
- (49) Önal, Y.; Akmil-Başar, C.; Sarıcı-Özdemir, Ç. Investigation Kinetics Mechanisms of Adsorption Malachite Green onto Activated Carbon. *J. Hazard. Mater.* **2007**, *146* (1–2), 194–203.
- (50) Gemeinhart, R. A.; Park, H.; Park, K. Pore Structure of Superporous Hydrogels. *Polym. Adv. Technol.* **2000**, *11* (8–12), 617–625.
- (51) Zhu, H.; Jia, Y.; Wu, X.; Wang, H. Removal of Arsenic from Water by Supported Nano Zero-Valent Iron on Activated Carbon. *J. Hazard. Mater.* **2009**, *172* (2–3), 1591–1596.
- (52) Zheng, M.; Lian, F.; Zhu, Y.; Zhang, Y.; Liu, B.; Zhang, L.; Zheng, B. PH-Responsive Poly (Xanthan Gum-g-Acrylamide-g-Acrylic Acid) Hydrogel: Preparation, Characterization, and Application. *Carbohydr. Polym.* **2019**, *210*, 38–46.